

pubs.acs.org/Macromolecules Article

# Efficient Polymerization of Methyl- $\varepsilon$ -Caprolactone Mixtures To Access Sustainable Aliphatic Polyesters

Derek C. Batiste, Marianne S. Meyersohn, Annabelle Watts, and Marc A. Hillmyer\*



Cite This: https://dx.doi.org/10.1021/acs.macromol.0c00050



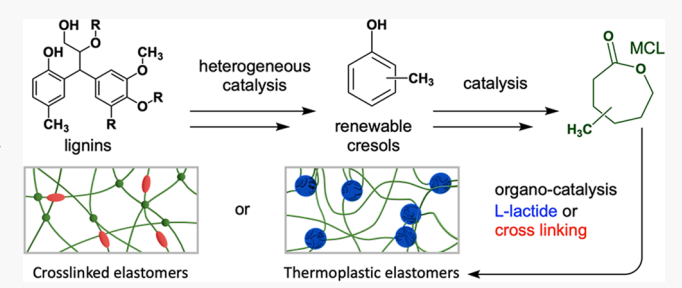
**ACCESS** 

III Metrics & More

Article Recommendations

Supporting Information

**ABSTRACT:** Aliphatic polyesters are a versatile class of materials that can be sourced from bioderived feedstocks. Poly( $\gamma$ -methyl- $\varepsilon$ -caprolactone) (P $\gamma$ MCL) in particular can be used to make degradable thermoplastic elastomers with outstanding mechanical properties. P $\gamma$ MCL can potentially be manufactured economically from p-cresol, a component of lignin bio-oils. A complication is that additional manufacturing processes are necessary to isolate pure cresol isomers. Using mixed feedstocks of cresol isomers to access the corresponding methyl-substituted  $\varepsilon$ -caprolactone (MCL) monomer mixtures would convey economic advantages



to sourcing these materials sustainably. Moreover, the use of organocatalysts in lieu of traditional tin-based catalysts averts issues with potential environmental and human toxicity. With these motivations in mind, we explored the ring-opening transesterification polymerization (ROTEP) of MCL mixtures and characterized the molecular, thermal, and rheological properties of the resulting copolymers. The molar mass of MCL mixtures that would be obtained from *meta*- and *para*-cresol can be readily modulated. The thermal and rheological properties of these statistical copolymers and terpolymers are at parity with pure  $P\gamma$ MCL homopolymer. The use of diphenyl phosphate (DPP) and dimethyl phosphate (DMP) as organocatalysts enabled access to these materials that have potential to improve sustainability in the synthesis of these polyesters.

# **■ INTRODUCTION**

Ring-opening polymerization (ROP) of lactones has proven instrumental in the synthesis of sustainable aliphatic polyesters with attractive and competitive material properties when compared to petrochemically derived analogues. The uses for these polymers include tough thermoplastic elastomers, polyurethane foams, thermosets, elastomers, and block copolymer-based micelles.<sup>1–5</sup> Given their versatility, there is a need to better understand how next-generation aliphatic polyesters are sourced and manufactured. Poly( $\gamma$ -methyl- $\varepsilon$ caprolactone) (PγMCL) has been employed for many of these applications due in large part to favorable polymerization kinetics and thermodynamics via metal-catalyzed ROP of  $\gamma$ methyl- $\varepsilon$ -caprolactone ( $\gamma$ MCL), a low entanglement molar mass  $(M_e)$ , and potential biodegradability.<sup>2,3</sup> Moreover, several researchers have invoked facile retrosynthetic routes that would enable access to \( \gamma MCL \), among other valuable molecules, from sustainable biomass-derived feedstocks.<sup>6–9</sup> In particular, lignin represents an enticing starting material due to its abundant supply and a surfeit of sources that generate it as a by-product of industrial scale processes, such as paper pulp refining and the lignocellulose-to-ethanol process. <sup>10,11</sup> Lignin bio-oils are the depolymerization products of lignins and are complex mixtures, comprised of hundreds of phenolic and cyclic aromatic compounds, the composition of which varies widely depending on such factors as lignin feedstock type, depolymerization method, heating rate, reaction temperature,

and catalysts. <sup>12</sup> These complexities have presented significant challenges in valorizing lignins as starting materials for the manufacture of commodity chemicals. <sup>13</sup>

Cresols are a class of chemicals that are components of lignin bio-oils. A significant fraction of the current global production infrastructure for cresols is designed to separate them from complex alkyl-phenol and alkoxy-phenol mixtures. So-called "natural" cresols are those isolated from coal tars and spent refinery caustics and make up 40% of global cresol production as recently as 2012.14 A key feature of natural cresol production is that only o-cresol is purified by fractional distillation, while the m-cresol and p-cresol isomers are recovered as a single fraction due to the close proximity of their boiling points. 15 To purify these isomers, further processes are necessary, for which several methods have been developed, including high-pressure crystallization via the Finecry process in Japan, <sup>16</sup> continuous flow adsorption via the Cresex process in the United States, <sup>17</sup> and alkylation using isobutene and acidic catalysts followed by fractional distillation and dealkylation in Germany. 14,18 In particular, p-cresol can serve as an efficient and highly economical starting material in

Received: January 8, 2020 Revised: February 7, 2020



the production of  $\gamma$ MCL, as demonstrated by a recent technoeconomic analysis by Lundberg et al. <sup>19</sup> The use of P $\gamma$ MCL to make mechanically robust materials has been well explored recently; however, the utilization of other poly(methyl- $\varepsilon$ -caprolactone)s (PMCLs) has received significantly less attention. <sup>6,20</sup>

Use of organotin and tin-based complexes as coordinationinsertion polymerization catalysts has become ubiquitous in both academe and industry. In particular, tin(II) catalysts have gained favor due to high efficiency, good polymerization control, and regulatory approval for use in food, medical, and pharmaceutical applications in many countries. 21,22 However, organotin compounds have been implicated to have several harmful effects in animals and the environment including cytotoxicity, endocrine disruption, and proteasome inhibition. 23-28 These factors have evoked criticism when materials synthesized with tin-based catalysts have been promulgated as sustainable and biodegradable, largely stemming from the fact that the inorganic element containing catalyst complexes are not typically removed in industrial polymer manufacturing. 23,29 An alternative that has garnered a great deal of attention in recent years has been the use of Brønsted acids to catalyze the ring-opening transesterification polymerization (ROTEP) of lactones. 30-33 Many researchers have proposed an activated monomer mechanism (AMM) for these reactions, a process that follows a living polymerization scheme. In particular, several phosphoric acid derivatives are efficacious in the polymerization of  $\varepsilon$ -caprolactone with quantitative conversions and good polymerization control.<sup>34,33</sup>

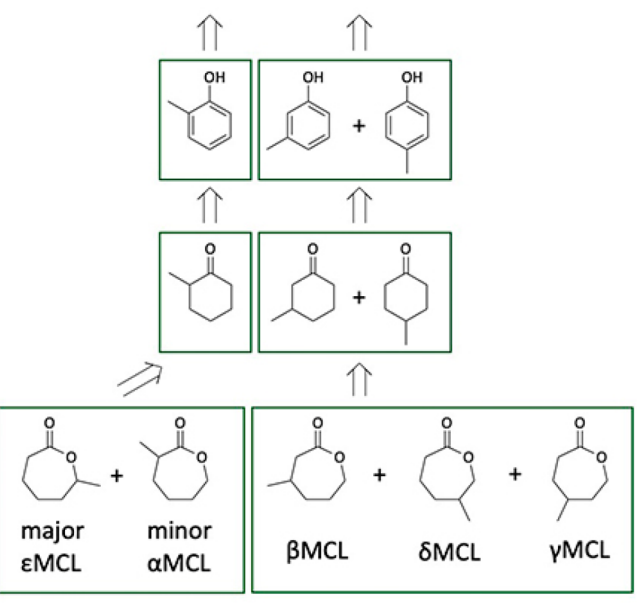
There are numerous challenges to overcome in the transition to a sustainable plastics economy.<sup>36</sup> The most daunting of these stems from the fact that the processes and manufacturing infrastructure for valorizing petroleum have been integrated and iterated upon for over a century, leading to highly streamlined and economical systems. For sustainable alternatives to be viable, the materials need to be both highperforming and economically sourced and manufactured. While several drop-in replacement monomers from biomass have been reported in recent years, economical manufacturing processes for these alternatives remain a challenge.<sup>37</sup> However, the use of renewably sourced p-cresol as a starting material to prepare  $\gamma$ MCL on a large scale appears to be promising. <sup>19</sup> Moreover, the manufacturing infrastructure to acquire cresols from coke-oven tars and other spent refinery caustics can feasibly be applied to lignin bio-oils because each of these raw materials is largely composed of alkyl- and alkoxyphenolic compounds in addition to cyclic and heterocyclic aromatics. 14,43,44

The motivation to industrially manufacture  $\gamma$ MCL is due to the discovery that P $\gamma$ MCL has thermal and rheological characteristics that lead to outstanding mechanical properties in elastomers. Previous work in our group has demonstrated that poly(methyl- $\delta$ -valerolactone)s also exhibit similar structure—property relationships. These results led us to hypothesize that statistical copolymers or terpolymers obtained from polymerizing mixtures of MCL isomers would also exhibit these desirable structure—property relationships due to the structural similarity between the polymer repeat units in comparison to previously studied materials (e.g., mono-methyl-substituted aliphatic ester repeat units). In addition to illuminating potential effects of regioisomerism on structure—property relationships of PMCL copolymers and terpolymers, we were also interested in the mechanistic

insights that these reactions could provide in the context of the AMM. In particular, we sought to understand how the position of the methyl substituent would affect the reaction rate, copolymer microstructure, and polymer properties. If PMCL copolymers exhibit the same rheological and thermal properties as  $P\gamma$ MCL, there are significant potential economic advantages for using mixed cresol feedstocks as starting materials to access this class of polymers. To wit, PMCL polymers would be economically advantageous for making strong, biodegradable, and sustainable materials because the additional processing and manufacturing measures needed to purify *meta*- and *para*-cresol would not be necessary (Scheme 1).

Scheme 1. Conversion of Lignin Bio-Oil Derived Cresols to Methyl-Substituted  $\varepsilon$ -Caprolactone Mixtures

# LIGNIN BIO-OIL



In this work, we report the organocatalytic ROTEP of methyl-substituted  $\varepsilon$ -caprolactone mixtures. We discuss the kinetics observed using diphenyl phosphate (DPP) as an organocatalyst and 1,4-benzenedimethanol (BDM) as the initiator in the context of the proposed AMM. We then characterize and compare the thermal and rheological properties of PMCL copolymers to PγMCL (e.g., glass transition temperature  $(T_g)$ , temperature at the onset of mass loss  $(T_{d,5\%})$ , and entanglement molar mass  $(M_e)$ ). Additionally, we report the use of dimethyl phosphate (DMP) as the organocatalyst for these systems, and the implications its use has on sustainability in polymer synthesis. Lastly, previous work from our group reported that triblock copolymers comprised of poly(L-lactide) as hard end blocks and PyMCL as the soft midblock functions as highly resilient and mechanically competitive thermoplastic elastomers (TPEs).2 Herein, we report the organocatalytic synthesis of these materials in the neat state using DPP as a catalyst to synthesize the PγMCL midblock and 1,8-diazabicyclo[5.4.0]undec-7-ene (DBU) to catalyze the synthesis of poly(L-lactide) end blocks.

Scheme 2. Proposed Brønsted Acid-Catalyzed Activated Monomer Mechanism of γMCL Using Diphenyl Phosphate<sup>a</sup>

"ROH (shown in green) represents an alcohol group on the initiator or the alcohol end group of the growing polymer chain.

Table 1. ROTEP of Methyl-Substituted ε-Caprolactones with Diphenyl Phosphate and 1,4-Benzenedimethanol<sup>a</sup>

						molar mass (kg/mol)			
sample	M:I	M:Cat	monomer feed ratio	time (h)	conv. <sup>b</sup> (%)	theor.c	$M_{ m n, \ NMR}^{d}$	$M_{\rm w,\;LS\;SEC}^{e}$	$D_{ m LS~SEC}$
$P(\gamma MCL)$ -10	78:1	83:1		65	95	10	10	11	1.2
$P(\gamma MCL)$ -25	196:1	97:1		21	98	25	27	28	1.1
$P(\gamma MCL)$ -51	401:1	75:1		65	>99	51	49	43	1.3
$P(\beta\delta MCL)$ -11	85:1	62:1	1:1	65	98	11	10	12	1.1
$P(\beta\delta MCL)$ -26	200:1	92:1	1:1	23	>99	26	27	27	1.1
$P(\beta\delta MCL)$ -52	405:1	95:1	1:1	65	>99	52	72	45	1.2
$P(\beta\delta MCL)$ -59 (100 °C)	459:1	98:1	1:1	2.5	98	59	69	57	1.4
$P(\beta\gamma\delta MCL)$ -11	85:1	107:1	1:1:1	51	>99	11	10	15	<1.1
$P(\beta\gamma\delta MCL)$ -28	209:1	101:1	1:1:1	51	>99	28	34	27	1.1
$P(\beta\gamma\delta MCL)$ -50	403:1	103:1	1:1:1	51	96	50	59	48	1.1
$P(\beta\gamma\delta MCL)$ -200	1583:1	96:1	1:1:1	144	>99	203	203	100	1.3
$P(\alpha \varepsilon MCL)$ -48	394:1	95:1	49:1	142	95	48	46	16	1.1

"Polymerizations were performed in neat monomer at ambient room temperature unless otherwise specified. Conversion determined with  $^1H$  NMR spectroscopy using mid-group analysis, assuming one initiator per chain. Theoretical  $M_{\rm n}$  calculations based on observed monomer conversion and the monomer to initiator ratio.  $^dM_{\rm n}$  determined with  $^1H$  NMR spectroscopy using mid-group analysis, assuming one initiator per chain.  $^eM_{\rm w,\ LS\ SEC}$  determined using multiple angle laser light scattering size exclusion chromatography (MALLS-SEC) with THF as the mobile phase.

# ■ RESULTS AND DISCUSSION

Molar Mass Control. The use of Brønsted acids to catalyze the ROTEP of lactones has been reported extensively in recent years. 30,31,35,46 These polymerizations are proposed to proceed according to the AMM (Scheme 2). In addition to activating monomer, researchers have provided computational evidence suggesting that DPP acts as a bifunctional catalyst in these systems, both activating monomer and exogenous alcohol initiator via hydrogen bonding. AMM polymerizations follow a living polymerization scheme, where a chain growth polymerization occurs in the absence of significant termination and chain transfer reactions. This platform has enabled access to a myriad of well-defined polymer structures with control-

lable molar masses and narrow molar mass dispersity without the use of metal-based catalysts. The results of the ROTEP of a series of MCL compositions using DPP are shown in Table 1. When the monomer feed is composed of pure  $\gamma$ MCL, an equimolar mixture of  $\beta$ MCL and  $\delta$ MCL, or an equimolar mixture of  $\beta$ MCL,  $\gamma$ MCL, and  $\delta$ MCL, the  $M_n$  and  $M_w$  can be modulated by altering the monomer to initiator ratio in the feed. Additionally, the polymerization appears to follow a controlled scheme, with a linear increase in molar mass with increasing conversion and low molar mass dispersity at conversions <90% (Figure 1). The increase in molar mass dispersity at high conversion is likely due to transesterification

reactions that begin to compete when the monomer concentration is low. 48

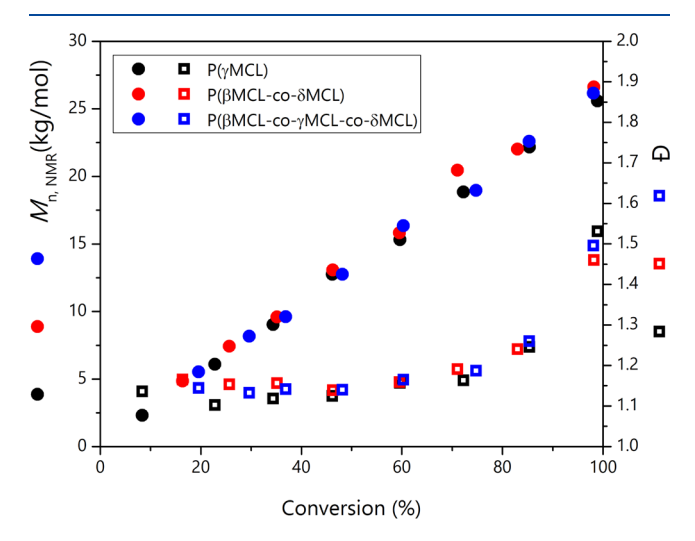


Figure 1.  $M_{\rm n}$  and  $\mathcal D$  vs conversion for methyl-substituted ε-caprolactone polymerizations using 1 mol % DPP at 100 °C. The theoretical  $M_{\rm n}$  at 100% conversion was 25 kg/mol for each experiment, based on the starting monomer to initiator ratio. Equimolar mixtures of monomers were used for copolymerizations and terpolymerizations.  $M_{\rm n}$  and conversion were measured using midgroup analysis, assuming one initiator per chain via <sup>1</sup>H NMR spectroscopy.  $\mathcal D$  was measured using SEC equipped with an RI detector calibrated with narrow dispersity polystyrene standards with chloroform as the mobile phase.

When a 49:1 mixture of  $\alpha$ MCL and  $\varepsilon$ MCL is polymerized with DPP, the  $M_{\rm w}$  does not exceed ~20 kg/mol, regardless of the monomer to initiator ratio (see Table 1, sample  $P(\alpha \varepsilon MCL)$ -48). In contrast, Martello et al. reported  $P\varepsilon MCL$ with molar masses >100 kg/mol via size exclusion chromatography (SEC) using tin(II) ethylhexanoate as the catalyst.<sup>6</sup> In addition to propagation, a potential side reaction for the secondary alcohol end group resulting from ring opening of  $\varepsilon$ MCL is an acid-mediated elimination reaction (Scheme 3). Elimination reactions such as these would yield olefins near the terminal end of the chain, resulting in chains that can no longer undergo monomer propagation. Evidence for this can be seen in the <sup>1</sup>H nuclear magnetic resonance (NMR) spectrum of a crude  $\alpha MCL/\epsilon MCL$  copolymerization reaction, in which resonances are present in the olefin region (see the Supporting Information, Figure S7). Additionally, these reactions result in the production of water as a by-product in the reaction, which can act as an adventitious initiator and further limits the maximum molar mass achievable.

We hypothesized that steric factors would render the AMM of  $\alpha$ MCL and  $\epsilon$ MCL difficult due to the proximity of the methyl substituent to the ester bond. Specifically, in  $\alpha$ MCL, the methyl substituent directly adjacent to the carbonyl carbon could hinder the attack of a hydroxyl end group on a polymer chain. In the case of  $\epsilon$ MCL, ring opening results in a secondary alcohol end group, which should be significantly more hindered in reacting with an activated carbonyl than the primary alcohol end group of the other MCL monomers. These steric factors can be used to rationalize the slower observed polymerization rate in  $\alpha$ MCL/ $\epsilon$ MCL copolymerizations (Figure 2).

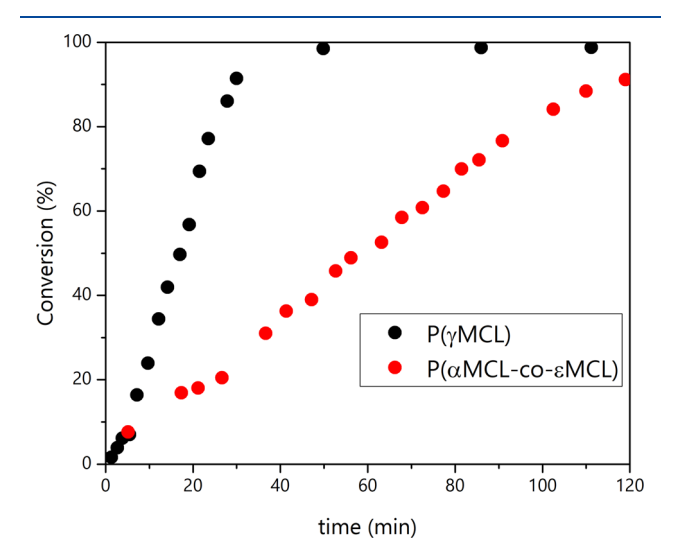


Figure 2. Conversion vs time plots for ROTEP of γMCL and a 49:1 mixture of εMCL and αMCL. Polymerizations were conducted at 100 °C with 1 mol % DPP under a nitrogen atmosphere using standard glovebox techniques. The theoretical  $M_{\rm n}$  at 100% conversion was 25 kg/mol for each experiment, based on the starting monomer to initiator ratio. Conversion was measured with <sup>1</sup>H NMR spectroscopy by removing aliquots quenched with CDCl<sub>3</sub> containing ~0.5 mg/mL pyridine.

# Polymerization Kinetics Using Diphenyl Phosphate.

Given that the molar masses can be easily modulated for mixtures of  $\beta$ MCL,  $\gamma$ MCL, and  $\delta$ MCL, we investigated the differences in the rates of polymerization for pure  $\gamma$ MCL compared to the MCL mixtures. Figure 3 shows the plots of conversion versus time for the polymerization of pure  $\gamma$ MCL, an equimolar mixture of  $\beta$ MCL and  $\delta$ MCL, and an equimolar mixture of  $\beta$ MCL,  $\gamma$ MCL, and  $\delta$ MCL. For each monomer composition, near-quantitative conversion was reached in <60 min using 1 mol % DPP as a catalyst at 100 °C. A key feature

Scheme 3. Possible Side Reaction in ROTEP of  $\alpha$ MCL and  $\varepsilon$ MCL<sup> $\alpha$ </sup>

"We depict an E1 elimination reaction of 2° alcohol end group in DPP-catalyzed ROTEP of εMCL (see the Supporting Information, Figure S7).

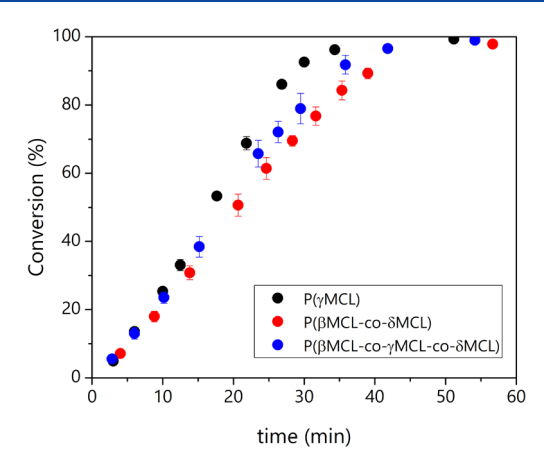


**Figure 3.** Conversion vs time plots for the ROTEP of γMCL, a 1:1 mixture of βMCL and δMCL, and a 1:1:1 mixture of βMCL, γMCL, and δMCL. Each experiment was performed in triplicate. Data points are the average of the data, and error bars represent the standard deviation. Polymerizations were conducted at 100 °C with 1 mol % DPP under a nitrogen atmosphere using standard glovebox techniques. The theoretical  $M_{\rm n}$  at 100% conversion was 25 kg/mol for each experiment, based on the starting monomer to initiator ratio. Conversion was measured with  $^1$ H NMR spectroscopy by removing aliquots quenched with CDCl<sub>3</sub> containing ~0.5 mg/mL pyridine.

of these results is that the rate of monomer consumption is essentially linear over the course of a majority of the reaction, implying that the rate of polymerization does not appreciably slow down even as the [M] is decreasing. This feature is indicative of a rate law that is zero or pseudo-zero order in monomer concentration ([M]). This deviation from first-order kinetics mirrors the results reported for the DPP-catalyzed ROTEP of other cyclic esters.  $^{30,35}$ 

While conventional living polymerizations that typically proceed by first-order kinetics are generally well understood, the kinetic scheme for AMM polymerizations is more complex. There have been mixed reports on the dependence of [M] in the observed rate law for AMM polymerizations of cyclic esters. In 2006, Baśko and Kubisa reported a distinct first-order dependence on [M] for the AMM polymerization of L-lactide in DCM using triflic acid; however, a significant deviation from first-order kinetics was observed when  $\varepsilon$ -caprolactone was used as the monomer. 49 In 2011, Makiguchi et al. reported distinct first-order dependences on [M] using DPP as the catalyst for the bulk polymerization of  $\delta$ -valerolactone and  $\varepsilon$ -caprolactone.<sup>34</sup> Conversely, Delcroix et al. later reported a deviation from first-order kinetics for DPP and diphenyl phosphoramidic acid-catalyzed polymerizations of  $\varepsilon$ -caprolactone in toluene.<sup>35</sup> In 2013, Makiguchi et al. reported a distinct first-order dependence in [M] for the DPP-catalyzed bulk AMM polymerization of trimethylene carbonates. 50 Recently, Schneiderman et al. reported a pseudo-zero-order dependence on [M] in the DPP-catalyzed bulk polymerization of a bevy of alkyl-substituted  $\delta$ -valerolactones. A detailed analysis on the complexity of AMM polymerization kinetics was provided by Basko and Kubisa. The propagation reaction in AMM polymerization is dependent on the concentration of protonated monomer ( $[M - H^{+}]$ ), which is not necessarily related to the instantaneous [M] alone. As the polymerization proceeds, the protic acid catalyst can protonate a monomer, an ester in the polymer backbone, a hydroxyl end group, or a deprotonated catalyst. Thus, there are numerous equilibria involved, and the  $[M - H^{+}]$  can be expressed as

$$[M - H^{+}] = \frac{[H^{+}][M]}{[M] + [P]\frac{K_{p}}{K_{m}} + [ROH]\frac{K_{ROH}}{K_{m}} + [DPP^{-}]\frac{K_{D}}{K_{m}}}$$

where  $[H^+]$  is the overall proton concentration; [P] is the concentration of polymer repeat units; [M] is the concentration of monomer; [ROH] is the concentration of hydroxyl groups;  $[DPP^-]$  is the concentration of the deprotonated catalyst; and  $K_p$ ,  $K_m$ ,  $K_{ROH}$ , and  $K_D$  are the equilibrium constants for protonation of the polymer ester group, monomer, hydroxyl group, and deprotonated catalyst, respectively. If the basicity of the monomer and polymer ester group is equal, then  $K_p/K_m \approx 1$ , and the balance of the components of the equation is constant. The expression then becomes

$$[M - H^{\dagger}] = A[M] \tag{2}$$

where A is the constant

$$\frac{[H^{+}]}{[M] + [P] + [ROH] \frac{K_{ROH}}{K_{m}} + [DPP^{-}] \frac{K_{D}}{K_{m}}}$$
(3)

Note that although [P] and [M] change over time, [P] + [M] is assumed to always be constant. Thus, an integrated rate law can be written where a first-order plot of  $\ln[M_0]/[M]_t$  versus time should be linear. However, when  $K_p/K_m \neq 1$ , [M – H<sup>+</sup>] is not directly proportional to [M], and a downward or upward deflection is observed in the semilogarithmic coordinates when trying to model the kinetics by a first-order process.

The complexity of the kinetics observed in the Brønsted acid-catalyzed AMM deepens further as one considers the case of copolymerizations and terpolymerizations. Under a terminal control mechanism, the relative incorporation of comonomers in a conventional chain-growth polymerization is dictated by the propagation rate constants for each unique chain end with each comonomer and the ratio of the concentrations of comonomers. In the case of AMM copolymerizations, the ratio of the protonated comonomer concentrations becomes the critical variable, which, like the homopolymerization case, may not be correlated to the concentrations of the comonomers alone. If one comonomer is more basic, then it should be protonated preferentially and thus be preferentially incorporated into the copolymer. The data on relative basicity of methyl-substituted lactones is limited; however, we hypothesized that the relative basicity between  $\beta$ MCL,  $\gamma$ MCL, and  $\delta$ MCL would not differ greatly and would yield statistical copolymers with some distribution of each monomer present at each section of the polymer chains. Analysis of the discrete conversion of  $\beta$ MCL and  $\delta$ MCL for a polymerization of an equimolar mixture of the two monomers can be found in the "Copolymer composition" section of the Supporting Informa-

Kinetic data for the polymerization of pure  $\gamma$ MCL, an equimolar mixture of  $\beta$ MCL and  $\delta$ MCL, and an equimolar mixture of  $\beta$ MCL,  $\gamma$ MCL, and  $\delta$ MCL in semilogarithmic coordinates are shown in Figure 4. The upward curvature observed in each of these experiments indicates that  $K_p/K_m$  is not equal to 1 in these cases and that the basicity of each monomer ester is higher than the basicity of each resulting ester unit in the polymer chain, consistent with previous observations of higher basicities of lactones compared to linear

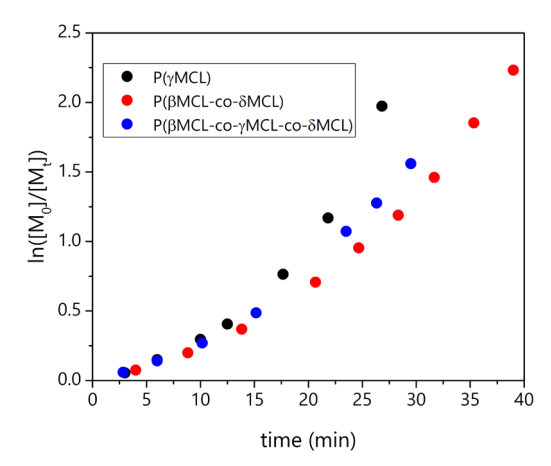


**Figure 4.** Kinetic data for ROTEP of pure γMCL, 1:1 mixture of βMCL and δMCL, and 1:1:1 mixture of βMCL, γMCL, and δMCL in semilogarithmic coordinates. Polymerizations were conducted at 100 °C with 1 mol % DPP under a nitrogen atmosphere using standard glovebox techniques. The theoretical  $M_{\rm n}$  at 100% conversion was 25 kg/mol for each experiment, based on the starting monomer to initiator ratio. Conversion was measured with ¹H NMR spectroscopy by removing aliquots quenched with CDCl<sub>3</sub> containing ~0.5 mg/mL pyridine.

esters. This result suggests that  $[M-H^+]$  decreases at a slower rate relative to [M] over the course of the polymerizations, which leads to an apparent acceleration as the reaction proceeds and an apparent zero-order dependence on [M] in the rate law. These results are consistent with results reported by Schneiderman and Hillmyer, Delcroix et al., and Baśko and Kubisa for the AMM polymerization of  $\varepsilon$ -caprolactone,  $\delta$ -valerolactones, and alkyl-substituted  $\delta$ -valerolactones. Future studies correlating the basicity of monomers with reactivity ratios in AMM copolymerizations and terpolymerizations may shed more light on the mechanistic details of these reactions.

To investigate the dependence of [DPP] in these reactions, we conducted several kinetics experiments at varying catalyst concentrations while fixing the [M]:[ROH] ratio. Table 2 shows the rate constants for the polymerizations of each monomer set at 100 °C for varying concentrations of DPP. Each rate constant was calculated using data collected before reaching 90% conversion, which was approximated as the linear region of the reaction. Under these conditions, the observed rate constants  $(k_{obs})$  increase with increasing [DPP] and the observed order for [DPP] in the rate law for each monomer composition is 0.8. Previous kinetic investigations in ROTEP of methyl-substituted  $\delta$ -valerolactone using alcohol initiators and DPP as the catalyst reported fractional orders in [DPP] and [ROH] in the observed rate law. 30 Similarly, we also observe fractional dependences for [DPP] and [ROH] for each monomer composition. Further results and analysis can be found in the "Data Analysis" section of the Supporting Information.

Another potential mechanism for polymerization of heterocyclic monomers with protonic acid catalysts is the active chain-end (ACE) mechanism. In the ACE mechanism, initiation and propagation occur via the nucleophilic attack on an activated monomer or active chainend by a monomer molecule (Scheme 4). Conversely, initiation and propagation in the AMM occur via the nucleophilic attack on an activated monomer by an exogenous

Table 2. Rate Data for ROTEP of MCLs Using Varying Concentrations of DPP

sample (polymer)	$\frac{k_{\mathrm{obs}}^{}a}}{(\mathrm{M/h})}$	[DPP] <sub>0</sub> <sup>b</sup>	[BDM] <sub>0</sub> <sup>b</sup>	$M_n^c$ (kg/mol)	$t_{1/2}^{d}$ (min)
$P(\gamma MCL)$	2.1	7.5	41	22	114
$P(\gamma MCL)$	8.4	42	41	24	28
$P(\gamma MCL)$	16	82	41	25	15
$P(\gamma MCL)$	25	159	41	25	9.6
$P(\gamma MCL)$	41	243	41	26	5.8
$P(\beta MCL$ -co- $\delta MCL)$	2.3	12	41	21	104
$P(\beta MCL$ -co- $\delta MCL)$	6.6	43	41	23	36
$P(\beta MCL$ -co- $\delta MCL)$	11	82	41	24	22
$P(\beta MCL$ -co- $\delta MCL)$	20	163	41	26	12
$P(\beta MCL$ -co- $\delta MCL)$	28	242	41	25	8.5
P( $\beta$ MCL-co- $\gamma$ MCL-co- $\delta$ MCL)	2.3	11	41	21	104
$P(\beta MCL$ - $co$ - $\gamma MCL$ - $co$ - $\delta MCL)$	7.2	43	41	25	33
$P(\beta MCL$ - $co$ - $\gamma MCL$ - $co$ - $\delta MCL)$	13	82	41	24	18
$P(\beta MCL$ - $co$ - $\gamma MCL$ - $co$ - $\delta MCL)$	20	161	41	25	12
$P(\beta MCL$ - $co$ - $\gamma MCL$ - $co$ - $\delta MCL)$	32	242	41	25	7.5

"Rate constants calculated based on the observed pseudo-zero-order rate in monomer concentration. Kinetic experiments were performed in triplicate, and rate constants were calculated based on the average of the data. <sup>b</sup>Concentrations in mmol. <sup>c</sup>M<sub>n</sub> determined using midgroup analysis via <sup>1</sup>H NMR spectroscopy. <sup>d</sup>Time required for 50% conversion calculated using initial monomer concentration and observed rate constant.

initiator or the chain end (i.e., exogenous alcohol or hydroxyl end groups) (Scheme 2). Assuming the monomer is sufficiently more basic than the alcohol, when it is added to an ACE-controlled polymerization, an alcohol merely acts as a chain transfer agent, with no appreciable influence on the rate of polymerization. <sup>54</sup> Under AMM-controlled polymerizations, the exogenous alcohol serves as the initiator and the initial concentration of ROH groups is presumably proportional to the concentration of active chain ends (hydroxyl end groups). Thus, in AMM-controlled polymerizations, the rate of polymerization is, in part, proportional to the initial concentration of exogenous alcohol.

To investigate the influence of [ROH] on the rate of polymerization of MCL, we conducted kinetic experiments at varying initiator concentrations while fixing the [M]:[DPP] ratio. Table 3 shows the rate constants for the polymerizations of each monomer set at 100 °C for varying concentrations of BDM. Under these conditions, the observed rate constants  $(k_{\text{obs}})$  increase with increasing [BDM]. For the polymerization of  $\gamma$ MCL, the observed order for [ROH] in the rate law is 0.8. For the copolymerization  $\beta$ MCL and  $\delta$ MCL and the terpolymerization of  $\beta$ MCL,  $\gamma$ MCL, and  $\delta$ MCL, the observed order for [ROH] in the rate law is 0.6. These results strongly support the hypothesis that MCL polymerizations with DPP proceed according to the AMM. The fractional orders observed for [DPP] and [ROH] may be due to multiple competing protonation/deprotonation equilibria under the differing conditions, potential dimerization as a result of hydrogen bonding between two catalyst species, and potential adventitious initiation from residual water contamination in the catalyst. The practical outcome of these studies is the knowledge of how to reproducibly prepare PMCLs with target

### Scheme 4. ACE Polymerization Scheme of γMCL

$$A^{\odot}$$
 +  $A^{\odot}$  +  $A^{\odot}$ 

Table 3. Rate Data for ROTEP of MCLs Using Varying Concentrations of BDM

cample (melymen)	$\frac{k_{\rm obs}^{a}}{({\rm M/h})}$	[DPP] <sub>0</sub> <sup>b</sup>	[BDM] <sub>0</sub> <sup>b</sup>	$M_n^c$	$t_{1/2}^{d}$
sample (polymer)	(IVI/II)	$[DPP]_0$		(kg/mol)	(min)
$P(\gamma MCL)$	12	81	51	4.9	20
$P(\gamma MCL)$	19	81	68	10	13
$P(\gamma MCL)$	24	81	100	14	10
$P(\gamma MCL)$	38	81	203	19	6.2
$P(\beta MCL$ -co- $\delta MCL)$	14	81	51	4.9	17
$P(\beta MCL$ -co- $\delta MCL)$	17	81	68	9.8	14
$P(\beta MCL$ -co- $\delta MCL)$	23	81	104	15	10
$P(\beta MCL-co-\delta MCL)$	25	81	204	18	9.6
$P(\beta MCL$ - $co$ - $\gamma MCL$ - $co$ - $\delta MCL)$	16	81	51	4.9	15
P( $\beta$ MCL-co- $\gamma$ MCL-co- $\delta$ MCL)	19	81	68	9.8	13
$P(\beta MCL$ - $co$ - $\gamma MCL$ - $co$ - $\delta MCL)$	25	81	101	14	9.6
P( $\beta$ MCL-co- $\gamma$ MCL-co- $\delta$ MCL)	37	81	200	18	6.5

"Rate constants calculated based on the observed pseudo-zero-order rate in monomer concentration. Kinetic experiments were performed in triplicate, and rate constants were calculated based on the average of the data.  $^b\mathrm{Concentrations}$  in mmol.  $^cM_\mathrm{n}$  determined using midgroup analysis via  $^1\mathrm{H}$  NMR spectroscopy.  $^d\mathrm{Time}$  required for 50% conversion calculated using initial monomer concentration and observed rate constant.

molar masses and expected polymerization times. Further analysis can be found in the "Data Analysis" section of the Supporting Information.

Polymerization Kinetics and Polymer Purification Using Dimethyl Phosphate. Metal-based catalysts are highly prevalent in the production of several classes of commodity synthetic polymer materials. <sup>29,55,56</sup> Developments in the field of catalysis over the past century have generated many catalysts with incredibly high efficiency and selectivity, features which enable industrial scale production with very low catalyst concentrations. Subsequently, the use of killing agents to "quench" or deactivate catalysts is favored in polymer manufacturing because this prevents depolymerization and other unbidden reactions after the polymer has been processed into its consumer-ready form. 57,58 Depolymerization is particularly perilous because it can drastically alter the material's properties and incorporate monomers into the product, which can be toxic.<sup>59</sup> While advantageous from a process perspective, residual metal contaminants create a litany of issues in materials that require biocompatibility or microelectronic applications. 60-63 Additionally, there is added concern pertaining to leaching of potentially toxic additives (e.g., catalyst complexes, fillers, and stabilizers) because a significant percentage of synthetic polymers escapes waste management systems and end up in the environment.<sup>64–66</sup>

Devolatilization serves as one of the primary methods to purify industrial synthetic polymers by removing residual volatiles (e.g., solvents, monomer, and trapped air) once the reaction is complete. This process does not typically remove organometallic catalysts or the catalyst–killing agent complexes. In contrast, volatile organocatalysts can potentially be removed by the devolatilization process, thereby eliminating catalyst contamination in the final material, mitigating concerns about leaching and/or depolymerization. These factors motivated us to explore the use of dimethyl phosphate (DMP) as the ROTEP catalyst for  $\gamma$ MCL. DMP is a commercially available acid (p $K_a \approx 1.3$  in water) that is a liquid at room temperature with a boiling point of 174 °C. That is a liquid at room temperature with a boiling point of 174 °C. That is a liquid at for the DMP-catalyzed ROTEP of  $\gamma$ MCL is shown in Figure 5. Surprisingly, the reaction takes ~4.2 h to approach

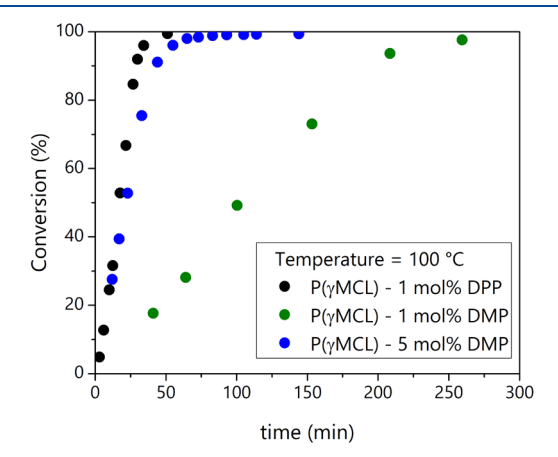


Figure 5. Conversion vs time for the ROTEP of γMCL catalyzed by 1 and 5 mol % DMP and 1 mol % DPP at 100 °C. The theoretical  $M_{\rm n}$  at 100% conversion was 25 kg/mol for each experiment, based on the starting monomer to initiator ratio. Conversion was measured with <sup>1</sup>H NMR spectroscopy by removing aliquots quenched with CDCl<sub>3</sub> containing ~0.5 mg/mL pyridine.

quantitative conversion, nearly 6× longer than the DPP-catalyzed polymerization at the same catalyst loading, despite higher reported p $K_a$  values for DPP (boiling point, 378 °C; p $K_a$ , 2–4). While there is variation in the conditions under which the p $K_a$ 's for the two phosphoric acid derivatives were measured and reported, similar results were reported by Gazeau-Bureau et al., wherein methane sulfonic acid was just as active catalytically as triflic acid in the ROTEP of  $\varepsilon$ -caprolactone, despite a p $K_a$  difference over 10 units.

The  $^1$ H NMR spectra of a ROTEP reaction of  $\gamma$ MCL using 4.3 mol % DMP at 100  $^{\circ}$ C is shown in Figure 6. The bottom spectrum indicates that the polymerization reaches near-quantitative conversion after 2.1 h at this increased catalyst loading level. The top spectrum is the reaction mixture after the polymerization vessel was subjected to reduced pressure

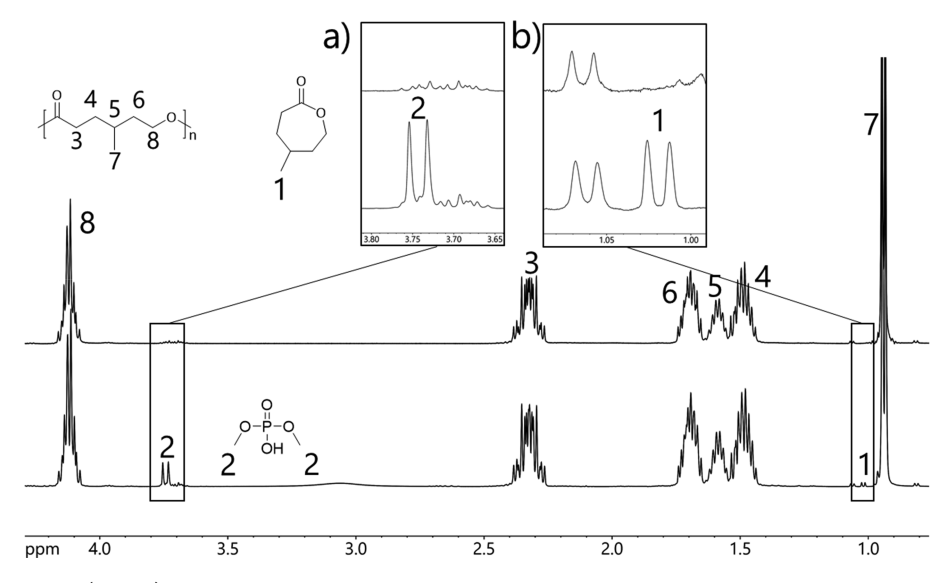


Figure 6. Devolatilization of  $P(\gamma MCL)$  synthesized with DMP. The bottom spectrum shows the crude polymerization reaction after 2.1 h with 4.3 mol % DMP at 100 °C (quenched in CDCl<sub>3</sub> containing ~0.4 mg/mL pyridine). The top spectrum is the polymerization reaction after 2 h under vacuum at 200–50 mTorr and 100 °C. Inset (a) shows near-quantitative removal of the DMP catalyst. Inset (b) shows near-quantitative removal of residual monomer.

(50 mTorr) at 100 °C for 2 h. Insets (a and b) show that this treatment results in near-quantitative removal of both residual monomer and DMP catalyst. A system such as this has the potential to improve the sustainability of conventional polymer synthesis, both industrially and academically. 1,78 Despite lower activity, ROTEP of \( \gamma \text{MCL} \) using DMP can be performed on the same timescale as DPP by simply increasing the catalyst loading. Industrially, this is typically not ideal for the environmental and toxicity related concerns mentioned previously, as well as possible changes in material properties associated with higher concentrations of impurities. However, for this system, these concerns are allayed because DMP is readily removed by the devolatilization process, which effectively enables genuine, facile polymer purification. When this treatment is applied to a polymerization using DPP, the catalyst is not removed by devolatilization and thus, a marked drop in  $M_n$  is observed due to the continuous removal of monomer following depolymerization as the monomer concentration drops below the equilibrium monomer concentration (Figure 7).

In academic settings, polymers are very commonly purified via successive precipitations. This procedure requires significant amounts of solvent in relation to the amount of polymer and several hours to days of drying time. As we have demonstrated, a system wherein the devolatilization step also removes catalyst enables polymer purification in a matter of hours, without use of solvent. Additionally, recovery and reuse of catalysts confers other practical advantages when designing sustainable processes. The <sup>1</sup>H NMR spectra of the reuse of DMP are shown in Figure 8. The bottom spectrum is the distillate of a polymerization of  $\gamma$ MCL using 2 mol % DMP with BDM as an initiator. The principal components of this mixture are DMP and residual \( \gamma MCL \) monomer. This recovered DMP/γMCL mixture was combined with a fresh solution of  $\gamma$ MCL and BDM, transferred to a polymerization vessel, and sealed under a nitrogen atmosphere. The top spectrum shows that quantitative conversion of  $\gamma$ MCL to PγMCL is achieved after 17.5 h at 100 °C. This demonstrates the continued activity of the recovered DMP and suitability for

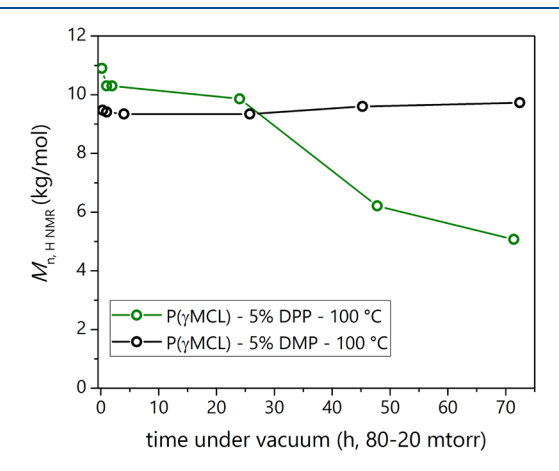


Figure 7. Devolatilization of P( $\gamma$ MCL) synthesized with DMP and DPP. Each reaction was run in a sealed polymerization vessel with a Schlenk adapter under a nitrogen atmosphere at 100 °C for 1 h. When the reaction was complete, the Schlenk adapter was opened to vacuum (80–20 mTorr). Aliquots were acquired by placing the reaction under positive argon pressure before unsealing the vessel.  $M_{\rm n}$  was measured using mid-group analysis via  $^{1}$ H NMR spectroscopy, assuming one initiator per chain.

catalyst recycling, a feature that further improves and enables sustainability in polymer synthesis.

Synthesis of High Molar Mass PMCL and Limitations of DMP. A critical parameter that drastically impacts the mechanical properties of elastomers is the molar mass of the constituent polymers. Previous work from our group investigated triblock polymer TPEs, which employ  $P\gamma MCL$  as a soft midblock and semicrystalline P(L-lactide) as the hard end blocks. Results from these studies showed that these materials are high-performing, strong, and resilient materials when the  $P\gamma MCL$  molar mass is in the range of  $50-100 \text{ kg/mol.}^2$  When DPP is used as the catalyst, polymers with a weight-average molar mass above 100 kg/mol can be accessed (Table 1 and Figure 5). When DMP is used as the catalyst, the weight-average molar masses deviate sharply from the

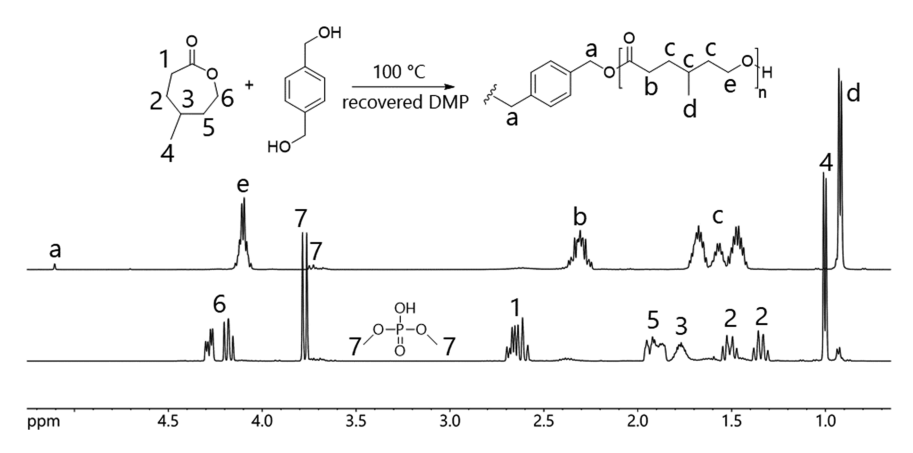


Figure 8. Devolatilization and reuse of DMP. The bottom spectrum is the distillate recovered from a  $P(\gamma MCL)$  polymerization using 2 mol % DMP. The distillate was recovered at 100 °C and 500 mTorr using a Kugelrohr distillation apparatus. The top spectrum shows the polymerization of a solution of γMCL and BDM after mixing with the distillate shown in the bottom spectrum. Conversion was >95% after 17.5 h at 100 °C.

Table 4. ROTEP of Methyl-Substituted  $\varepsilon$ -Caprolactones with Varying Monomer to Initiator Ratios and Varying Monomer to Catalyst Ratios Using DMP<sup>a</sup>

							molar mass (kg/mol)			
sample (polymer- $M_{\rm n,theo}$ )	M:I	M:Cat	temp. ( $^{\circ}$ C)	time (h)	conv. <sup>b</sup> (%)	theor. $^{c}$	$M_{\rm n, \ NMR}^{d}$	$M_{ m n, \ RI \ SEC}^{e}$	$M_{ m w,\;LS\;SEC}^{f}$	$\mathcal{D}_{\mathrm{RI}\;\mathrm{SEC}}^{\mathbf{g}}$
$P(\gamma MCL)$ -25	198:1	99:1	100	4.32	98	31	22	23	24	1.6
$P(\gamma MCL)$ -44	350:1	65:1	RT	124	99	44	13	18	27	1.7
$P(\gamma MCL)$ -99	790:1	35:1	100	4.28	98	99	90	22	37	2.0
$P(\gamma MCL)$ -C	n/a <sup>h</sup>	101:1	100	22.6	>99	n/a <sup>h</sup>	38 <sup>i</sup>	22	41	2.0

"Polymerizations were performed under a nitrogen atmosphere in a glovebox. b Conversion determined with  $^1H$  NMR spectroscopy using midgroup analysis, assuming one initiator per chain. Theoretical  $M_{\rm n}$  calculations based on observed monomer conversion and the monomer to initiator ratio.  $^dM_{\rm n}$  determined with  $^1H$  NMR spectroscopy using mid-group analysis, assuming one initiator per chain.  $^eM_{\rm n,\,RI\,SEC}$  determined using SEC with a refractive index (RI) detector with THF as the mobile phase.  $^fM_{\rm w,\,LS\,SEC}$  determined using MALLS-SEC with THF as the mobile phase. B was measured using RI-SEC calibrated with narrow dispersity polystyrene standards with chloroform as the mobile phase.  $^hn/a$ , not applicable.  $^tM_{\rm n,\,NMR}$  value is an estimation calculated using end group analysis. The putative end group resonances at  $\sim 3.7$  ppm (Figure 10) are assumed to be the result of only hydroxyl end groups.

I

theoretical values when targeting molar masses above ~25 kg/ mol (Table 4). Recently, there has been some controversy regarding the potential for phosphoric acid derivatives to act as both catalysts and initiators in AMM polymerizations.<sup>79–83</sup> Lewinski et al. showed that DPP and di-o-tolyl phosphate (DTP) efficiently catalyze the polymerization of  $\varepsilon$ -caprolactone without the addition of exogenous alcohol initiator. The results of their investigation determined that polymerization was initiated by residual water contamination in the catalysts, even after rigorous attempts to dry the materials via sublimation and successive lyophilizations.<sup>83</sup> However, it was postulated that other protonic acids with low steric bulk and suitable acidity could potentially act as both a catalyst and an initiator. Given the strong deviation in theoretical and observed molar mass when using DMP to target high molar mass polymers (see Table 4, P( $\gamma$ MCL)-99), we investigated the reaction of  $\gamma$ MCL with DMP without an exogenous alcohol initiator to determine if water, DMP initiation, or other potential side reactions were the cause.

When  $\gamma$ MCL was combined with 1 mol % DMP without an added initiator, quantitative conversion to polymer was observed after 22.6 h at 100 °C. Additionally, unlike the characteristic linear increase in conversion over time observed previously with BDM added as an initiator (Figures 3 and 6), the rate of the polymerization appears to accelerate slightly before the reaction reaches equilibrium (Figure 9). To investigate the structure of the end groups, the reaction mixture was devolatilized for 15 h at 100 °C to remove the

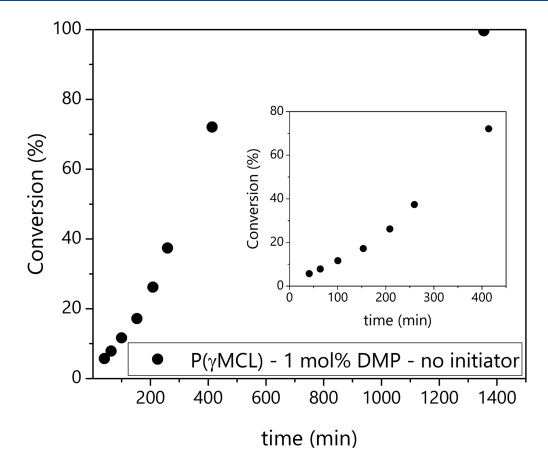


**Figure 9.** Conversion vs time for the polymerization of  $\gamma$ MCL catalyzed by 1 mol % DMP at 100 °C without an exogenous initiator. The inset shows time points below 80% conversion. Conversion was measured with <sup>1</sup>H NMR spectroscopy by removing aliquots quenched with CDCl<sub>3</sub> containing ~0.5 mg/mL pyridine.

catalyst and then purified further by precipitation. The putative end group resonances in the  $^1H$  NMR spectra were compared to the corresponding resonances of purified P $\gamma$ MCL made with 1 mol % DPP without an exogenous alcohol initiator. Figure 10 shows the end group resonances of the purified P $\gamma$ MCL made with 1 mol % DMP. Upon the addition of trifluoroacetic anhydride (TFA), a majority of the end group resonances shift

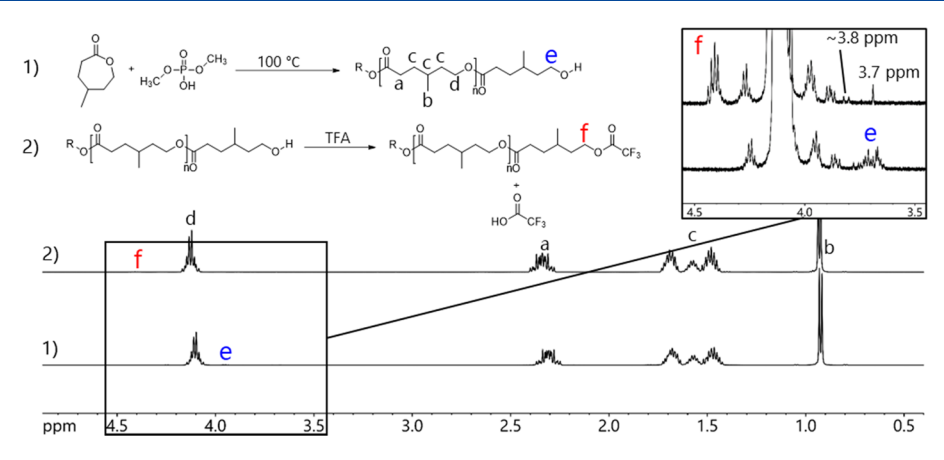


Figure 10. <sup>1</sup>H NMR investigation of the end group structure of  $P\gamma$ MCL synthesized with 1 mol % DMP at 100 °C and without an exogenous initiator. The bottom spectrum is  $P\gamma$ MCL after devolatilization for 15 h and 30 mTorr followed by precipitation into hexanes and drying in vacuo. The top spectrum is the sample of  $P\gamma$ MCL in the bottom spectrum after the addition of 2 drops of TFA.

downfield from ~3.7 to ~4.4 ppm, indicative of hydroxylfunctionalized end groups converting to trifluoromethyl ester end groups via esterification. The resonances remaining in the original end group region are a doublet at ~3.8 ppm and a singlet at 3.7 ppm. The coupling constant for the doublet at  $\sim$ 3.8 ppm (I = 11.5 Hz) is the same as the doublet observed in the <sup>1</sup>H NMR spectrum of DMP (Figure S37). Additionally, the chemical shift of the singlet at 3.7 ppm corresponds closely with the singlet observed at 3.66 ppm in PyMCL synthesized with 1 mol % DPP and 6 mol % methanol as the exogenous alcohol initiator; this singlet being assigned as a methyl ester end group (Figure S36). Conversely, when TFA is added to purified PyMCL made with 1 mol % DPP and no exogenous alcohol initiator, all of the end group resonances shift downfield to ~4.4 ppm, indicative of complete hydroxyl end group functionality (Figure 10 and Figure S35). In light of the previously discussed investigation by Lewinski et al. on DPPcatalyzed polymerization of  $\varepsilon$ -caprolactone, these results are consistent with water contamination in DMP and DPP, acting as an initiator in the polymerization of MCLs. Additionally, other end groups are present as additional side reactions can occur when using DMP: potentially elimination of methanol, adventitious initiation by catalyst species, or reaction of catalyst species with hydroxyl end groups. Each of these potential side reactions is a probable cause for the observed disparity between the theoretical and observed molar masses.

To investigate catalyst stability, DMP was heated at 100 °C in the absence of both monomer and initiator. After 36 h, new resonances are observed in the <sup>1</sup>H, <sup>13</sup>C, and <sup>31</sup>P NMR spectra of the reaction mixture (Figures S37-S42). The small singlet at 3.49 ppm in the <sup>1</sup>H NMR spectrum is likely due to methanol, formed from a potential nucleophilic attack by water on the phosphorus in DMP followed by elimination of methanol (see Scheme S1 for other possibilities). Methanol can initiate the polymerization of MCL, leading to a methyl ester end group, a potential explanation for the singlet observed at 3.7 ppm (Figure 10). Other reactions between catalysts at this temperature can lead to the formation of phosphoric acid or methyl dihydrogen phosphate, resulting in catalyst species with additional acidic protons, species which can potentially be more active than DMP alone, potentially explaining the observed acceleration in the rate of polymerization before the reaction reaches equilibrium (Figure 9).

To investigate the potential for DMP to act as an initiator or react with the hydroxyl end group of a polymer chain, γMCL and DMP were reacted together in a 2:1 mole ratio at 100 °C for 30 min followed by devolatilization at 40 mTorr for 3 h. The products were then analyzed by matrix-assisted laser desorption ionization time-of-flight mass spectrometry (MALDI-TOF MS) in the positive reflector mode using potassium trifluoroacetate as the positive ion salt (Figures S43 and S44). The spectral analysis data show several signals, which closely correspond in mass to a wide variety of potential reaction products, including PyMCL initiated by water, PγMCL initiated by methanol, cyclic oligomerization, chain coupling, PyMCL initiated by DMP or nucleophilic attack on DMP by a hydroxyl end group followed by elimination of methanol or water, and condensation between two DMP molecules to form a phosphoanhydride followed by the attack of a hydroxyl chain end among others. Table S1 lists the proposed product structures for several potential reactions with corresponding theoretical molar masses and signals observed in Figure S44.

These results suggest that high molar mass PMCL polymers with high end group fidelity are difficult to synthesize using DMP at 100 °C. While molar mass control can be achieved up to ~25 kg/mol with 1 mol % DMP, extended reaction times or high catalyst loadings and elevated temperatures lead to unbidden side reactions that depress the observed molar mass when targeting high molar mass polymers. Conversely, polymers with molar masses >100 kg/mol have been synthesized using DPP. A potential strategy for accessing even higher molar masses for these polymers, first reported by Lewinski et al., would be to conduct the polymerization at an exceedingly high monomer to catalyst ratio and forgo the addition of exogenous alcohol initiator, relying solely on trace water present in the catalyst to initiate polymerization.<sup>83</sup> Although high molar mass may not be achieved with DMP, there are advantages in purification and sustainability that provide a promising alternative for use in making low molar mass aliphatic polyesters, which are commonly employed for a myriad of applications such as thermoplastic and chemically cross-linked polyurethane materials, chemically cross-linked elastomers, thermoset resins, thermally mendable materials, and materials with shape memory properties. 1,3,79,84-86

Thermal and Rheological Characterization. The most salient physical properties for soft TPE midblock candidates

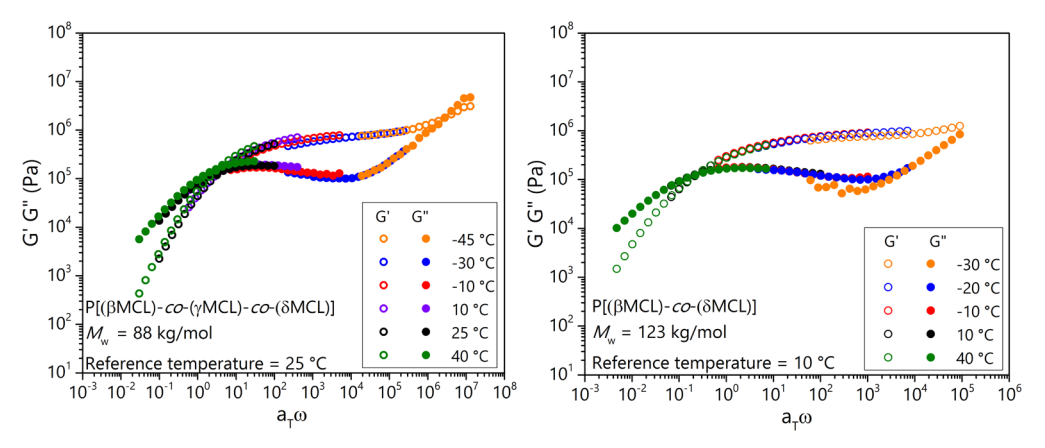


Figure 11. Master curves for P( $\beta$ MCL-co- $\delta$ MCL) and P( $\beta$ MCL-co- $\gamma$ MCL-co- $\delta$ MCL). Curves were acquired by applying shift factors ( $a_t$ ) to dynamic frequency sweep data. The reference temperatures are 10 °C for P( $\beta$ MCL-co- $\delta$ MCL) and 25 °C for P( $\beta$ MCL-co- $\gamma$ MCL-co- $\delta$ MCL).

are the entanglement molar mass  $(M_{\rm e})$  and glass transition temperature  $(T_{\rm g})^{.87}$  Several researchers have used P $\gamma$ MCL to make thermoplastic elastomer materials with excellent strength, toughness, and elasticity due in large part to the relatively low  $M_{\rm e}$  of P $\gamma$ MCL. $^{2,3,45}$  A comparison of the DMTA for high molar mass samples of P $[(\beta$ MCL)-co- $(\delta$ MCL)] and P $[(\beta$ MCL)-co- $(\gamma$ MCL)-co- $(\delta$ MCL)] revealed that the two polymers have similar plateau moduli to each other and P $\gamma$ MCL (Figure 11). $^2$  The  $M_{\rm e}$  for each of these copolymers was calculated using plateau modulus values determined from minima of the shifted tan  $\delta$  curves (see the Supporting Information, Figures S33 and S34). The  $T_{\rm g}$  and temperature at 5% mass loss  $(T_{\rm d,5\%})$  were determined using differential scanning calorimetry and thermogravimetric analysis, respectively (Table 5). In comparison to the thermal and rheological

Table 5. Entanglement Molar Masses  $(M_e)$ , Glass Transition Temperatures  $(T_g)$ , and Temperature at 5% Mass Loss  $(T_{d,5\%})$  for PMCL Copolymers

sample	$M_{\rm e}~({\rm kg/mol})$	$T_{\rm g}$ (°C)	$T_{\rm d,5\%}$ (°C)
$P(\gamma MCL)$	2.9 <sup>a</sup>	$-58^{a}$	350
$P(\beta MCL$ -co- $\delta MCL)$	2.8	-58	370
$P(\beta MCL-co-\gamma MCL-co-\delta MCL)$	3.7	-55	345

 $^{a}$  Values reported by Watts et al.  $^{2}$   $M_{\rm e}$  estimated using the plateau in the storage modulus at the minimum of the tan  $\delta$  (see the Supporting Information).  $T_{\rm g}$  measured using differential scanning calorimetry.  $T_{\rm d,5\%}$  measured using thermal gravimetric analysis under a nitrogen atmosphere at 10  $^{\circ}$  C/min.

data reported for  $P\gamma MCL$  by Watts et al., the  $M_e$  and  $T_g$  values between pure  $P\gamma MCL$  and the PMCL copolymers and terpolymers studied here are at parity. These results suggest that PMCL polymers can impart the same material properties to elastomers as  $P\gamma MCL$ . Furthermore, using a mixed feed of MCL monomers represents a significant economic advantage when sourcing them from cresols on an industrial scale because m-cresol and p-cresol can be separated as a mixture from o-cresol via fractional distillation and would require no further purification processes.

**PMCL PLLA Block Polymer Synthesis.** While many studies have demonstrated the efficacy of DPP as a catalyst for ROTEP of a myriad of heterocyclic monomers, DPP has been shown to be relatively ineffective for the polymerization of lactide. TS,88 However, a number of successful organocatalytic strategies for this monomer have been developed, and in

particular, tertiary amines have been well explored for this highly industrially relevant monomer.  $^{31,89}$  In this work, we investigated the use of 1,8-diazabicyclo[5.4.0]undec-7-ene (DBU) for the polymerization of L-lactide from PMCL previously synthesized with DPP. The experiment was conducted in bulk under a nitrogen atmosphere using standard glovebox techniques. Amorphous P $\gamma$ MCL was combined with the solid L-lactide monomer via manual mixing with a metal spatula. Once combined, 5.6 mol % DBU (to L-lactide) was added. The reaction mixture was agitated once more and allowed to sit at room temperature for 3 h, with manual agitation occurring at  $\sim$ 1 and  $\sim$ 2 h. After 3 h, the conversion of L-lactide was 74% via  $^{1}$ H NMR spectroscopy. Figure 12

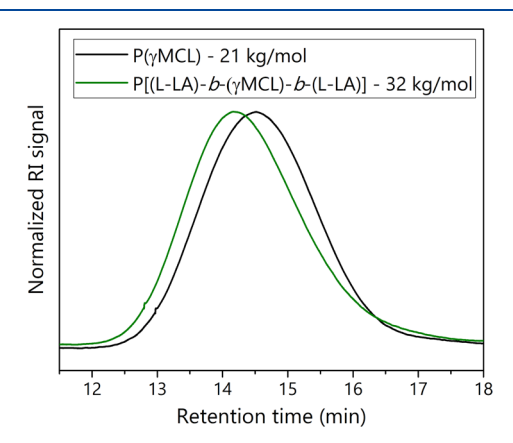


Figure 12. Chloroform SEC trace of P $\gamma$ MCL prepolymer and P(L-lactide-b- $\gamma$ MCL-b-L-lactide) copolymer synthesized with 5.5 mol % DBU (to L-lactide). The reaction was performed under a nitrogen atmosphere using standard glovebox techniques at room temperature in bulk for 3 h. The reaction mixture was agitated manually once per hour with a metal spatula.

shows the SEC traces of the starting  $P\gamma$ MCL and the block copolymer reaction after 3 h, indicating a marked increase in molar mass from an  $M_n$  of 21 to 32 kg/mol. Recently, one-pot approaches for the synthesis of multiblock copolymers have been reported. To explore the suitability of this approach for poly(L-lactide)-b-poly( $\gamma$ MCL)-b-poly( $\zeta$ -lactide), we synthesized a  $P\gamma$ MCL midblock using DPP and once the reaction was complete, L-lactide, DBU, and a small amount of toluene were added directly to the reaction vessel. Figure S49 shows the SEC traces of the starting  $P\gamma$ MCL and the block copolymer

after precipitation, indicating an increase in molar mass from an  $M_{\rm n}$  of 25 to 31 kg/mol. These results suggest that the tough, strong, and resilient poly(L-lactide)-b-poly( $\gamma$ MCL)-b-poly(L-lactide) TPEs we have reported in the past can be accessed with a one-pot strategy, organocatalytically, and without the use of solvents.

#### CONCLUSIONS

The results from this work demonstrate that DPP is an efficient and effective catalyst in the ROTEP of MCL mixtures. The molar masses of  $\gamma$ MCL and equimolar mixtures of  $\beta$ MCL,  $\gamma$ MCL, and  $\delta$ MCL can be easily modulated by changing the monomer to initiator ratio in the feed. The molar mass cannot be modulated in this way when  $\alpha$ MCL and  $\epsilon$ MCL are present due to termination reactions. The dependence of [M] in the observed rate law for these systems appears to be pseudo-zero order. The deviation from first-order kinetics mirrors many previous results for AMM polymerizations of cyclic esters and indicates that the basicity of  $\beta$ MCL,  $\gamma$ MCL, and  $\delta$ MCL is higher than the corresponding ester groups in the polymer. Future studies correlating  $pK_b$  values to reactivity ratios would likely provide further mechanistic insight into AMM copolymerizations. The use of DMP is also an effective organocatalytic strategy for the ROTEP of telechelic PMCL, albeit with significantly less activity and less control than DPP. The volatility of DMP enables facile polymer purification via devolatilization, which is beneficial in reducing contamination concerns in materials compared to current industrial polymerization practices.

The copolymers acquired from polymerizing equimolar mixtures of  $\beta$ MCL and  $\delta$ MCL or  $\beta$ MCL,  $\gamma$ MCL, and  $\delta$ MCL have comparable  $M_{\rm e}$  and  $T_{\rm g}$  values to P $\gamma$ MCL. The parity between the thermal and rheological properties of the PMCL copolymers with PyMCL suggest that they are also suitable for use in making materials with high mechanical strength, toughness, and elasticity. This indicates a significant economic advantage to using a mixed feed of MCL monomers versus pure \( \gamma \text{MCL} \), especially when sourcing them from cresols because the path from raw material to monomer is streamlined significantly by removing the need to separate m-cresol and pcresol isomers. This work demonstrates that high molar mass PMCL in the range of 50–100 kg/mol can be accessed in bulk at RT using DPP. Block copolymerization of L-lactide with PMCL can be accomplished in bulk, at room temperature and organocatalytically using DBU.

# ASSOCIATED CONTENT

# Supporting Information

The Supporting Information is available free of charge at https://pubs.acs.org/doi/10.1021/acs.macromol.0c00050.

Experimental details; instrumental details; further kinetics analysis; <sup>1</sup>H, <sup>13</sup>C, and <sup>31</sup>P NMR spectra, DMTA data, MALDI-TOF spectra, TGA data, DSC data, Table S1, Scheme S1, and Figures S1–S44 (PDF)

#### AUTHOR INFORMATION

#### **Corresponding Author**

Marc A. Hillmyer – Department of Chemistry, University of Minnesota, Minneapolis, Minnesota 55455-0431, United States; orcid.org/0000-0001-8255-3853;

Email: hillmyer@umn.edu

#### Authors

Derek C. Batiste — Department of Chemistry, University of Minnesota, Minneapolis, Minnesota 55455-0431, United States; orcid.org/0000-0001-6180-8749

Marianne S. Meyersohn — Department of Chemistry, University of Minnesota, Minneapolis, Minnesota 55455-0431, United States

Annabelle Watts — Department of Chemistry, University of Minnesota, Minneapolis, Minnesota 55455-0431, United States; © orcid.org/0000-0003-2310-3961

Complete contact information is available at: https://pubs.acs.org/10.1021/acs.macromol.0c00050

#### **Notes**

The authors declare no competing financial interest. All primary data files are available free of charge at https://doi.org/10.13020/wac6-s078.

## ACKNOWLEDGMENTS

We would like to acknowledge Dr. David Giles for advice on dynamic mechanical thermal analysis and Dr. Lucie Fournier for assistance with MALDI-TOF MS experiments. Additionally, we would like to acknowledge Dr. Chris DeRosa, Dr. Guilhem De Hoe, and Colin Peterson for helpful discussions. We would like to thank John Beumer for assistance creating the TOC graphic. We also acknowledge the funding for this work, which was provided by the NSF Center for Sustainable Polymers, CHE-1901635 at the University of Minnesota.

#### REFERENCES

- (1) Schneiderman, D. K.; Vanderlaan, M. E.; Mannion, A. M.; Panthani, T. R.; Batiste, D. C.; Wang, J. Z.; Bates, F. S.; Macosko, C. W.; Hillmyer, M. A. Chemically Recyclable Biobased Polyurethanes. *ACS Macro Lett.* **2016**, *5*, 515–518.
- (2) Watts, A.; Kurkokawa, N.; Hillmyer, M. A. Strong, Resilient, and Sustainable Aliphatic Polyester Thermoplastic Elastomers. *Biomacromolecules* **2017**, *18*, 1845–1854.
- (3) De Hoe, G. X.; Zumstein, M. T.; Tiegs, B. J.; Brutman, J. P.; McNeill, K.; Sander, M.; Coates, G. W.; Hillmyer, M. A. Sustainable Polyester Elastomers from Lactones: Synthesis, Properties, and Enzymatic Hydrolyzability. *J. Am. Chem. Soc.* **2018**, *140*, 963–973.
- (4) Xiao, Y.; Cummins, D.; Palmans, A. R. A.; Koning, C. E.; Heise, A. Synthesis of biodegradable chiral polyesters by asymmetric enzymatic polymerization and their formulation into microspheres. *Soft Matter* **2008**, *4*, 593–599.
- (5) Lee, R. S.; Huang, Y. T.; Chen, W. H. Synthesis and characterization of temperature-sensitive block copolymers from poly(N-isopropylacrylamide) and 4-methyl- $\varepsilon$ -caprolactone or 4-phenyl- $\varepsilon$ -caprolactone. *J. Apple. Polym. Sci.* **2010**, *118*, 1634–1642.
- (6) Martello, M. T.; Hillmyer, M. A. Polylactide-Poly(6-methyl-ε-caprolactone)-Polylactide Thermoplastic Elastomers. *Macromolecules* **2011**, 44, 8537–8545.
- (7) Van de Vyver, S.; Roman-Leshkov, Y. Emerging catalytic processes for the production of adipic acid. *Catal. Sci. Technol.* **2013**, 3, 1465–1479.
- (8) Schutyser, W.; Van Den Bosch, S.; Dijkmans, J.; Turner, S.; Meledina, M.; Van Tendeloo, G.; Debecker, D. P.; Sels, B. F. Selective Nickel-Catalyzed Conversion of Model and Lignin-Derivec Phenolic Compounds to Cyclohexanone-Based Polymer Building Blocks. *ChemSusChem* 2015, 8, 1805–1818.
- (9) Yakabi, K.; Mathieux, T.; Milne, K.; Lopez-Vidal, E. M.; Buchard, A.; Hammond, C. Continuous Production of Biorenewable, Polymer-Grade Lactone Monomers through Sn-β-Catalyzed Baeyer Villiger Oxidation with H2O2. *ChemSusChem* **2017**, *10*, 3652–3659. (10) Bu, Q.; Lei, H.; Zacher, A. H.; Wang, L.; Ren, S.; Liang, J.; Wei, Y.; Liu, Y.; Tang, J.; Zhang, Q.; Ruan, R. A review of catalytic

- hydrodeoxygenation of lignin-derived phenols from biomass pyrolysis. *Bioresour. Technol.* **2012**, *124*, 470–477.
- (11) Galbe, M.; Zacchi, G. Pretreatment of Lignocellulosic Materials for Efficient Bioethanol Production. In *Advances in Biochemical Engineering/Biotechnology: Biofuels*; Scheper, T.; Olsson, L. Ed.; Springer-Verlag: Berlin, 2007; Vol. 108; p 42.
- (12) Pandey, M. P.; Kim, C. S. Lignin Depolymerization and Conversion: A review of Thermochemical Methods. *Chem. Eng. Technol.* **2010**, 34, 29–41.
- (13) Sun, Z.; Fridrich, B.; de Santi, A.; Elangovan, S.; Barta, K. Bright Side of Lignin Depolymerization: Toward New Platform Chemicals. *Chem. Rev.* **2018**, *118*, 614–678.
- (14) Feige, H. Cresols and Xylenols. Ullmanns Encyclopedia of Industrial Chemistry, 2000.
- (15) Stevens, D. R. Separation of Individual Cresols and Xylenols from Their Mixtures. *Ind. Eng. Chem.* **1943**, *35*, 655–660.
- (16) Moritoki, M.; Kitagawa, K.; Onoe, K.; Kaneko, K. Process Technol, Proc. 1984, vol. 2, Ind. Crist., 377-380.
- (17) Neuzil, R. W.; Rosback, D. H.; Jensen, R. H.; Teague, J. R.; de Rosset, A. J. Chemtech 1980, 498-503.
- (18) Weinrich, W. Alkylated Cresols from Refinery Gases. *Ind. Eng. Chem.* **1943**, *35*, 264–272.
- (19) Lundberg, D. J.; Lundberg, D. J.; Hillmyer, M. A.; Dauenhauer, P. J. Techno-economic Analysis of a Chemical Process To Manufacture Methyl-*e*-caprolactone from Cresols. *ACS Sustainable Chem. Eng.* **2018**, *6*, 15316–15324.
- (20) Vion, J. M.; Jéoîme, R.; Teyssié, P. Synthesis, Characterization, And Miscibility of Caprolactone Random Copolymers. *Macromolecules* **1986**, *19*, 1828–1838.
- (21) Sobczak, M. Ring-Opening polymerization of cyclic esters in the presence of choline/SnOct2 catalytic system. *Polym. Bull.* **2012**, *68*, 2219–2228.
- (22) Evans, C. J. Chemistry of Tin; Springer: Dordrecht, 1998, 442–479.
- (23) Piver, W. T. Organotin Compounds: Industrial Applications and Biological Investigation. *Environ. Health Perspect.* **1973**, *4*, 61.
- (24) Álvarez-Chávez, C. R.; Edwards, S.; Moure-Eraso, R.; Geiser, K. Sustainability of bio-based plastics: general comparative analysis and recommendations for improvement. *J. Cleaner Prod.* **2012**, 23, 47–56.
- (25) Grün, F.; Watanabe, H.; Zamanian, Z.; Maeda, L.; Arima, K.; Cubacha, R.; Gardiner, D. M.; Kanno, J.; Iguchi, T.; Blumberg, B. Endocrine-disrupting organotin compounds are potent inducers of adipogenesis in vertebrates. *Mol. Endocrinol.* **2006**, *20*, 2141–2155.
- (26) Tanzi, M. C.; Verderio, P.; Lampugnani, M. G.; Resnati, M.; Dejana, E.; Sturani, E. Cytotoxicity of some catalysts commonly used in the synthesis of copolymers for biomedical use. *J. Mater. Sci.: Mater. Med.* **1994**, *5*, 393–396.
- (27) Cam, D.; Marucci, M. Influence of residual monomers and metals on poly(L-lactide) thermal stability. *Polymer* **1997**, *38*, 1879–1884.
- (28) Mori, T.; Nishida, H.; Shirai, Y.; Endo, T. Effects of chain end structures on pyrolysis of poly(l-lactic acid) containing tin atoms. *Polym. Degrad. Stab.* **2004**, *84*, 243–251.
- (29) Thiele, U. K. The Current Status of Catalysis and Catalyst Development for the Industrial Process of Poly(ethylene terephthalate) Polycondensation. *Int. J. Polym. Mater.* **2001**, *50*, 387–394.
- (30) Schneiderman, D. K.; Hillmyer, M. A. Aliphatic Polyester Block Polymer Design. *Macromolecules* **2016**, *49*, 2419–2428.
- (31) Kamber, N. E.; Jeong, W.; Waymouth, R. M. Organocatalytic Ring-Opening Polymerization. *Chem. Rev.* **2007**, *107*, 5813–5840.
- (32) Susperregui, N.; Delcroix, D.; Martin-Vaca, B.; Bourissou, D.; Maron, L. Ring-Opening Polymerization of  $\varepsilon$ -Caprolactone Catalyzed by Sulfonic Acids: Computational Evidence for Bifunctional Activation. *J. Org. Chem.* **2010**, *75*, 6581–6587.
- (33) Martin-Vaca, B.; Bourissou, D. Ring-opening Polymerization Promoted by Brønsted Acid Catalysts. In *Organic Catalysis for Polymerisation*; Dove, A.; Sardon, H.; Naumann, S. Eds.; RSC: London, 2019; pp 37–86.

- (34) Makiguchi, K.; Satoh, T.; Kakuchi, T. Diphenyl Phosphate as an Efficient Cationic Organocatalyst for Controlled/Living Ring-Opening Polymerization of  $\delta$ -Valerolactone and  $\varepsilon$ -Caprolactone. *Macromolecules* **2011**, *44*, 1999–2005.
- (35) Delcroix, D.; Couffin, A.; Susperregui, N.; Navarro, C.; Maron, L.; Martin-Vaca, B.; Bourissou, D. Phosphoric and phosphoramidic acids as bifunctional catalysts for the ring-opening polymerization of  $\varepsilon$ -caprolactone: a combined experimental and theoretical study. *Polym. Chem.* **2011**, *2*, 2249.
- (36) Schneiderman, D. K.; Hillmyer, M. A. 50th Anniversary Perspective: There Is a Great Future in Sustainable Polymers. *Macromolecules* **2017**, *50*, 3733–3749.
- (37) DeWilde, J. F.; Chiang, H.; Hickman, D. A.; Ho, C. R.; Bhan, A. Kinetics and Mechanism of Ethanol Dehydration on  $\gamma$ -Al2O3: The Critical Role of Dimer Inhibition. *ACS Catal.* **2013**, *3*, 798–807.
- (38) Williams, C. L.; Chang, C. C.; Do, P.; Nikbin, N.; Caratzoulas, S.; Vlachos, D. G.; Lobo, R. F.; Fan, W.; Dauenhauer, P. J. Cycloaddition of Biomass-Derived Furans for Catalytic Production of p-Xylene. *ACS Catal.* **2012**, *2*, 935–939.
- (39) Karp, E. M.; Eaton, T. R.; Sanchez, i.; Nogue, V.; Vorotnikov, V.; Biddy, M. J.; Tan, E. C. D.; Brandner, D. G.; Cywar, R. M.; Liu, R.; Manker, L. P.; Michener, W. E.; Gilhespy, M.; Skoufa, Z.; Watson, M. J.; Fruchey, O. S.; Vardon, D. R.; Gill, R. T.; Bratis, A. D.; Beckham, G. T. Renewable Acrylonitrile Production. *Science* **2017**, 358, 1307–1310.
- (40) Abdelrahman, O. A.; Park, D. S.; Vinter, K. P.; Spanjers, C. S.; Ren, L.; Cho, H. J.; Zhang, K.; Fan, W.; Tsapatsis, M.; Dauenhauer, P. J. Renewable Isoprene by Sequential Hydrogenation of Itaconic Acid and Dehydra-Decyclization of 3-Methyl-Tetrahydrofuran. *ACS Catal.* **2017**. 7, 1428–1431.
- (41) Makshina, E. V.; Dusselier, M.; Janssens, W.; Degreve, J.; Jacobs, P. A.; Sels, B. F. Review of old chemistry and new catalytic advances in the on-purpose synthesis of butadiene. *Chem. Soc. Rev.* **2014**, *43*, 7917–7953.
- (42) Buntara, T.; Noel, S.; Phua, P. H.; Melián-Cabrera, I.; de Vries, J. G. Caprolactam from Renewable Resources: Catalytic Conversion of 5-Hydroxymethylfurfural into Caprolactone. *Angew. Chem., Int. Ed.* **2011**, *50*, 7083–7087.
- (43) Zander, M. Aspects of Coal Tar Chemistry/A Review. *Polycyclic Aromat. Compd.* **1994**, *7*, 209–221.
- (44) Mullen, C. A.; Boateng, A. A. Catalytic pyrolysis-GC/MS of lignin from several sources. *Fuel Process. Technol.* **2010**, *91*, 1446–1458
- (45) Xiao, Y.; Lang, S.; Zhou, M.; Qin, J.; Yin, R.; Gao, J.; Heise, A.; Lang, M. A highly stretchable bioelastomer prepared by UV curing of liquid-like poly(4-methyl- $\varepsilon$ -caprolactone) precursors. *J. Mater. Chem. B* **2017**, *5*, 595–603.
- (46) Wang, H.; Wu, W.; Li, Z.; Zhi, X.; Chen, C.; Zhao, C.; Li, X.; Zhang, Q.; Guo, K. 2,4-Dinitrobenzenesulfonic acid in an efficient Brønsted acid-catalyzed controlled/living ring-opening polymerization of  $\varepsilon$ -caprolactone. *RSC Adv.* **2014**, *4*, 55716–55722.
- (47) Zhu, N.; Liu, Y.; Liu, J.; Ling, J.; Hu, X.; Huang, W.; Feng, W.; Guo, K. Organocatalyzed chemoselective ring-opening polymerizations. *Sci. Rep.* **2018**, *8*, 3734.
- (48) Martello, M. T.; Burns, A.; Hillmyer, M. Bulk Ring-Opening Transesterification Polymerization of the Renewable  $\delta$ -Decalactone Using an Organocatalyst. *ACS Macro Lett.* **2012**, *1*, 131–135.
- (49) Baśko, M.; Kubisa, P. Cationic copolymerization of  $\varepsilon$ -caprolactone and L,L-lactide by an activated monomer mechanism. *J. Polym. Sci., Part A: Polym. Chem.* **2006**, 44, 7071–7081.
- (50) Makiguchi, K.; Ogasawara, Y.; Kikuchi, S.; Satoh, T.; Kakuchi, T. Diphenyl Phosphate as an Efficient Acidic Organocatalyst for Controlled/Living Ring-Opening Polymerization of Trimethylene Carbonates Leading to Block, End-Functionalized, and Macrocyclic Polycarbonates. *Macromolecules* **2013**, *46*, 1772–1782.
- (51) Wiberg, K. B.; Waldron, R. F. Lactones. 3. A Comparison of the Basicities of Lactones and Esters. J. Am. Chem. Soc. 1991, 113, 7705–7709.

- (52) Kubisa, P.; Penczek, S. Cationic activated monomer polymerization of heterocyclic monomers. *Prog. Polym. Sci.* **1999**, *24*, 1409–1437.
- (53) Bednarek, M.; Kubisa, P.; Penczek, S. Coexistence of Activated Monomer and Active Chain End Mechanisms in Cationic Copolymerization of Tetrahydrofuran with Ethylene Oxide. *Macromolecules* 1999, 32, 5257–5263.
- (54) Kaluzynski, K.; Lewinski, P.; Pretula, J.; Szymanski, R.; Penczek, S.  $\varepsilon$ -Caprolactone Polymerization Catalyzed by Heteropolyacid. Derivation of the Kinetic Equation for Activated Monomer Propagation and Determination of the Rate Constants of Propagation. *Macromolecules* **2019**, *52*, 6405–6415.
- (55) National Research Council. Polymer Science and Engineering: The Shifting Research Frontiers; The National Academies Press: Washington, DC, 1994.
- (56) Kiparissides, C. Polymerization reactor modeling: A review of recent developments and future directions. *Chem. Eng. Sci.* **1996**, *51*, 1637–1659.
- (57) de Haan, I. A. B. *Process Technology: An Introduction*; Walter de Gruyter GmbH: Berlin/Boston, 2015.
- (58) Wagner, J. R., Jr. Multilayer Flexible Packaging: Technology and Applications for the Food, Personal Care and Over-The-Counter Pharmaceutical Industries; Elsevier: Oxford, 2010.
- (59) Moharamzadeh, K.; Van Noort, K.; Brook, I. M.; Scutt, A. M. Cytotoxicity of resin monomers on human gingival fibroblasts and HaCaT keratinocytes. *Dent. Mater.* **2007**, *23*, 40–44.
- (60) Miserque, O.; Brusselle, A.; Warichet, V. Process to Kill a Catalyzed Olefin Polymerization. US 20110190459A1, March 31, 2006.
- (61) Hedrick, J. L.; Magbitang, T.; Connor, E. F.; Glauser, T.; Volksen, W.; Hawker, C. J.; Lee, V. Y.; Miller, R. D. Application of Complex Macromolecular Architectures for Advanced Microelectronic Materials. *Chem. Eur. J.* **2002**, *8*, 3308–3319.
- (62) Albertsson, A. C.; Varma, I. K. Recent Developments in Ring Opening Polymerization of Lactones for Biomedical Applications. *Biomacromolecules* **2003**, *4*, 1466–1486.
- (63) Chemical Processing. Metal-Free Catalyst Enhances Polymerization. https://www.chemicalprocessing.com/articles/2017/metal-free-catalyst-enhances-polymerization/ (accessed Nov 10, 2018).
- (64) Ojeda, T. Polymers and the Environment. In *Polymer Science*; Yilmaz, F., Ed.; *Intech: London*, 2013; p 1.
- (65) Moore, C. J. Synthetic polymers in the marine environment: A rapidly increasing, long-term threat. *Environ. Res.* **2008**, 108, 131–130
- (66) World Economic Forum, Ellen MacArthur Foundation and McKinsey and Company, The New Plastics Economy Rethinking the Future of Plastics; 2016; [report] http://www.ellenmacarthurfoundation.org/publications.
- (67) Latinen, G. A. Devolatilization of Viscous Polymer Systems. In *Polymerization and Polycondensation Processes*; Platzer, N. A. J., Ed.; American Chemical Society: 1962; Vol. 34; p 235.
- (68) Albalak, R. Polymer Devolatilization; CRC Press: Boca Raton, 1996.
- (69) Tadmor, Z.; Gogos, C. G.; Principles of Polymer Processing; 2nd ed.; Wiley-Interscience: Hoboken, 2006.
- (70) Kumler, W. D.; Eiler, J. J. The Acid Strength of Mono and Diesters of Phosphoric Acid. The n-Alkyl Esters from Methyl to Butyl, the Esters of Biological Importance, and the Natural Guanidine Phosphoric Acids. J. Am. Chem. Soc. 1943, 65, 2355–2361.
- (71) Synquest Laboratories. Dimethyl hydrogen phosphate. http://synquestlabs.com/product/id/66448.html (accessed Nov 10, 2018).
- (72) Matrix Scientific. Dimethyl hydrogen phosphate, 95+%. http://www.matrixscientific.com/098585.html (accessed Nov 10, 2018).
- (73) Makiguchi, K.; Saito, T.; Satoh, T.; Kakuchi, T. Bis(4-nitrophenyl) phosphate as an efficient organocatalyst for ring-opening polymerization of  $\beta$ -butyrolactone leading to end-functionalized and diblock polyesters. *J. Polym. Sci., Part A: Polym. Chem.* **2014**, *52*, 2032–2039.

- (74) Saito, T.; Aizaway, Y.; Tajima, K.; Isono, T.; Satoh, T. Organophosphate-catalyzed bulk ring-opening polymerization as an environmentally benign route leading to block copolyesters, end-functionalized polyesters, and polyester-based polyurethane. *Polym. Chem.* **2016**, *6*, 4374–4384.
- (75) Christ, P.; Lindsay, A. G.; Vormittag, S. S.; Neudörfl, J. M.; Berkessel, A.; O'Donoghue, A. C. p*K*a Values of Chiral Brønsted Acid Catalysts: Phosphoric Acids/Amides, Sulfonyl/Sulfuryl Imides, and Perfluorinated TADDOLs (TEFDDOLs). *Chem. Eur. J.* **2011**, 8524–8528.
- (76) Chemenu, Inc. Diphenyl hydrogen phosphate, CM191860. https://www.chemenu.com/products/CM191860 (accessed Feb 6, 2020)
- (77) Gazeau-Bureau, S.; Delcroix, D.; Martin-Vaca, B.; Bourissou, D.; Navarro, C.; Magnet, S. Organo-Catalyzed ROP of  $\epsilon$ -Caprolactone: Methanesulfonic Acid Competes with Trifluoromethanesulfonic Acid. *Macromolecules* **2008**, *41*, 3782–3784.
- (78) Mezzasalma, L.; Harrisson, S.; Saba, S.; Loyer, P.; Coulembier, O.; Taton, D. Bulk Organocatalytic Synthetic Access to Statistical Copolyesters from L-Lactide and  $\varepsilon$ -Caprolactone Using Benzoic Acid. Biomacromolecules **2019**, 20, 1965–1974.
- (79) Torron, S.; Johansson, M. Oxetane-terminated telechelic epoxyfunctional polyesters as cationically polymerizable thermoset resins: Tuning the reactivity with structural design. *J. Polym. Sci., Part A: Polym. Chem.* **2015**, *53*, 2258–2266.
- (80) Cheng, G.; Fan, X.; Pan, W.; Liu, Y. Ring-opening polymerization of  $\varepsilon$ -caprolactone initiated by heteropolyacid. *J. Polym. Res.* **2010**, *17*, 847–851.
- (81) Basko, M.; Kubisa, P. Cationic polymerization of L, L-lactide. J. Polym. Sci., Part A: Polym. Chem. 2010, 48, 2650–2658.
- (82) Malik, P.; Chakraborty, D. Hydrogen phosphates: self-initiated organocatalysts for the controlled ring-opening polymerization of cyclic esters. *Inorg. Chim. Acta* **2013**, *400*, 32–41.
- (83) Lewinski, P.; Pretula, J.; Kaluzynski, K.; Kaźmierski, S.; Penczek, S. ε-Caprolactone: Activated monomer polymerization; controversy over the mechanism of polymerization catalyzed by phosphorous acids (diarylhydrogen phosphates). Do acids also act as initiators? *J. Catal.* **2019**, *371*, 305–312.
- (84) Schuh, C.; Schuh, K.; Lechmann, M. C.; Garnier, L.; Kraft, A. Shape-Memory properties of Segmented Polymers Containing Aramid Hard Segments and Polycaprolactone Soft Segments. *Polymer* **2010**, *2*, 71–85.
- (85) Nawaby, A. V.; Farah, A. A.; Liao, X.; Pietro, W. J.; Day, M. Biodegradable Open Cell Foams of Telechelic Poly( $\varepsilon$ -caprolactone) Macroligand with Ruthenium (II) Chromophoric subunits via Sun-Critical CO2 Processing. *Biomacromolecules* **2005**, *6*, 2458–2461.
- (86) Nguyen, L. T.; Nguyen, H. T.; Truong, T. T. Thermally mendable material based on a furyl-telechelic semicrystalline polymer and a maleimide crosslinker. *J. Polym. Res.* **2015**, 22, 186.
- (87) Tong, J. D.; Jerôme, Ř. Dependence of the Ultimate Tensile Strength of Thermoplastic Elastomers of the Triblock Type on the Molecular Weight between Chain Entanglements of the Central Block. *Macromolecules* **2000**, 33, 1479–1481.
- (88) Makiguchi, K.; Kikuchi, S.; Yanai, K.; Ogasawara, Y.; Sato, S.; Satoh, T.; Kakuchi, T. Diphenyl Phosphate/4-Dimethylaminopyridine as an Efficient Binary Organocatalyst System for Controlled/Living Ring-Opening Polymerization of L-Lactide Leading to Diblock and End-Functionalized Poly(L-Lactide)s. J. Polym. Sci., Part A: Polym. Chem. 2014, 52, 1047–1054.
- (89) Lohmeijer, B. G. G.; Pratt, R. C.; Leibfarth, F.; Logan, J. W.; Long, D. A.; Dove, A. P.; Nederberg, F.; Choi, J.; Wade, C.; Waymouth, R. M.; Hedrick, J. L. Guanidin and Amidine Organocatalysts for Ring-Opening Polymerization of Cyclic Esters. *Macromolecules* **2006**, *39*, 8574–8583.
- (90) Wang, X.; Liu, J.; Xu, S.; Xu, J.; Pan, X.; Liu, J.; Cui, S.; Li, Z.; Guo, K. Traceless switch organocatalysis enables multiblock ring-opening copolymerizations of lactones, carbonates, and lactides: by a one plus one approach in one pot. *Polym. Chem.* **2016**, *7*, 6297–6308.